

## Search for rare di-muon B-decays at ATLAS

---

**Iskander Ibragimov\*** on behalf of the ATLAS collaboration<sup>†</sup>

*University of Siegen, Walter-Flex-Str. 3, D57072 Siegen, Germany*

*E-mail: ibragimov@hep.physik.uni-siegen.de*

A search for the rare decay  $B_s^0 \rightarrow \mu^+ \mu^-$  has been performed in LHC proton-proton collisions at a center-of-mass energy of 7 TeV with the ATLAS detector using the first  $2.4 \text{ fb}^{-1}$  of data collected in 2011. The observed number of events is in agreement with the background expectation. The resulting upper limit on the branching fraction is  $\mathfrak{B}(B_s^0 \rightarrow \mu^+ \mu^-) < 2.2 (1.9) \times 10^{-8}$  at 95% (90%) confidence level.

*The XIth International Conference on Heavy Quarks and Leptons,  
June 11-15, 2012  
Prague, Czech Republic*

---

\*Speaker.

<sup>†</sup>This work was supported in part by BMBF.

## 1. Introduction

The  $B_s^0 \rightarrow \mu^+ \mu^-$  decay is a Flavor Changing Neutral Current (FCNC) process. It is strongly suppressed in the Standard Model (SM) and the theoretical prediction of its branching fraction is  $\mathfrak{B}(B_s^0 \rightarrow \mu^+ \mu^-) = (3.2 \pm 0.2) \times 10^{-9}$  [1]. A larger branching fraction would potentially indicate contributions from New Physics. Until now neither an enhancement of the branching fraction has been observed nor the theoretical limit has been reached experimentally [2, 3, 4, 5]. This paper describes the first measurement performed by the ATLAS experiment using the first  $2.4 \text{ fb}^{-1}$  of data collected in 2011 [6]. The ATLAS detector is described elsewhere [7]. A di-muon trigger with  $p_T > 4 \text{ GeV}$  for each of the two muon candidates was used to select events. The trigger conditions remained unchanged for the data sample used in the analysis; on the average 6 interactions per crossing have been observed.

## 2. Analysis Strategy

To be independent of the uncertainties of the luminosity and  $b\bar{b}$  production cross-section measurements, the branching fraction measurement is performed with respect to an abundant decay  $B^\pm \rightarrow J/\psi K^\pm$  ( $J/\psi \rightarrow \mu^+ \mu^-$ ):

$$\mathfrak{B}(B_s^0 \rightarrow \mu^+ \mu^-) = \frac{N_{\mu^+ \mu^-}}{N_{J/\psi K^\pm}} \times \frac{f_u}{f_s} \times \mathfrak{B}(B^\pm \rightarrow J/\psi K^\pm \rightarrow \mu^+ \mu^- K^\pm) \times \frac{\varepsilon_{J/\psi K^\pm} A_{J/\psi K^\pm}}{\varepsilon_{\mu^+ \mu^-} A_{\mu^+ \mu^-}},$$

where  $N$  is the number of observed events for each decay mode,  $f_u/f_s$  is the ratio of  $b$ -quark fragmentation fractions,  $\varepsilon$  and  $A$  are the absolute efficiency and the acceptance, respectively. The branching fraction, which would correspond to a single observed event, is defined as the Single Event Sensitivity (SES). The analysis is blind, i.e. the data from a di-muon invariant mass region of  $\pm 300 \text{ MeV}$  around the  $B_s^0$  mass is excluded from the optimization of the selection procedure. Instead, the  $B_s^0 \rightarrow \mu^+ \mu^-$  signal Monte Carlo (MC) and the background extrapolated from sidebands ( $4766 \text{ MeV} < m_{\mu^+ \mu^-} < 5066 \text{ MeV}$  and  $5666 \text{ MeV} < m_{\mu^+ \mu^-} < 5966 \text{ MeV}$ ) are used. The data sample is split into two parts: one half of the data is used for the selection optimization using a multivariate analysis technique and another half for the background measurement. For this analysis we take  $f_u/f_s = 0.267 \pm 0.021$  [8] assuming  $f_u = f_d$  [9] and no  $p_T$  or  $\eta$  dependence of the ratio. The yield  $N_{J/\psi K^\pm}$  is measured from data. The ratios of the efficiencies and the acceptances are estimated from MC samples, each  $\varepsilon \times A$  product being calculated as the ratio of the reconstructed and selected events to the number of generated events in the corresponding MC sample. The number of signal candidates  $N_{\mu^+ \mu^-}$  is counted after unblinding. The  $CL_s$  method [10] is used for the upper limit calculation.

The mass resolution and therefore the signal/background separation power of the ATLAS detector depends strongly on the pseudorapidity  $\eta$  of the reconstructed particles. Therefore data was split into 3 mass resolution categories separated by  $|\eta|_{max}$  of the two decay muons: 0-1 (60 MeV resolution), 1-1.5 (80 MeV resolution) and 1.5-2.5 (110 MeV resolution). The event selection was optimized separately for each category and the results are combined in the  $CL_s$  method.

### 3. Background Composition

The background comprises of continuous and resonant background components. The continuous background component originates from the random combination of muon tracks created in quark-anti-quark annihilation processes. These processes could be of prompt (e.g. Drell-Yan) or of non-prompt (dominated by  $b\bar{b} \rightarrow \mu^+ \mu^- X$  decays) origin. The resonant background comes from the decays of neutral  $B$ -mesons with one or two hadrons in the final state. For such decays one or both hadrons can be mis-identified as muons, mainly due to the punch-through of hadron to the ATLAS Muon Spectrometer or due to in-flight decays. The  $B \rightarrow hh$  background mimics the signal topology and therefore is hard to suppress. In the analysis, the contributions from the resonant decays were estimated from the dedicated MC sample using data-driven mis-identification rates and accounted for in the limit extraction.

### 4. Event Selection

For the selection of the  $B_s^0$  candidates several discriminating variables related to the primary and secondary vertices and to the decay muons have been calculated. From these, 14 variables with the highest discriminating power, which are not correlated to the di-muon mass and not strongly correlated to each other, were chosen as inputs for the multi-variate analysis. The variables [6] are listed below, where the vector  $\Delta\vec{x}$  is a vector from the primary vertex (PV) to the secondary vertex (SV) and the PV is chosen as the closest in  $z$  to the SV of the candidate:

- $|\alpha_{2D}|$  *pointing angle* - absolute value of the angle between  $\Delta\vec{x}$  and  $\vec{p}^B$  in the transverse plane,
- $\Delta R$  - angle  $\sqrt{(\Delta\phi)^2 + (\Delta\eta)^2}$  between  $\Delta\vec{x}$  and  $\vec{p}^B$ ,
- $L_{xy}$  *transverse decay length* - projection of  $\Delta\vec{x}$  onto  $\vec{p}_T^B$  direction,
- $ct$  *significance* - proper decay length  $ct = L_{xy} \times m_B / p_T^B$  divided by its uncertainty,
- $\chi_{xy}^2, \chi_z^2$  - vertex separation significance  $\Delta\vec{x}^T \cdot (\sigma_{\Delta\vec{x}}^2)^{-1} \cdot \Delta\vec{x}$  in  $(x, y)$  and  $z$ , respectively,
- $I_{0.7}$  *isolation* - ratio of  $|\vec{p}_T^B|$  to the sum of  $|\vec{p}_T^B|$  and the transverse momenta of all tracks, associated with the PV of the  $B$  candidate, with  $p_T > 0.5$  GeV within a cone  $\Delta R < 0.7$  from the  $B$  direction, excluding  $B$  decay products,
- $|d_0|^{\max}, |d_0|^{\min}$  - maximum and minimum values of the absolute transverse impact parameter of the two muon candidates relative to the PV,
- $|D_{xy}^{\min}|, |D_z^{\min}|$  - absolute values of the minimum distance of closest approach in the  $xy$  plane (or along  $z$ ) of tracks in the event to the  $B$  vertex,
- $p_T^B$  - transverse momentum of the  $B$  candidate,
- $p_L^{\max}, p_L^{\min}$  - maximum and minimum momentum of the two muon candidates along the  $B$  direction.

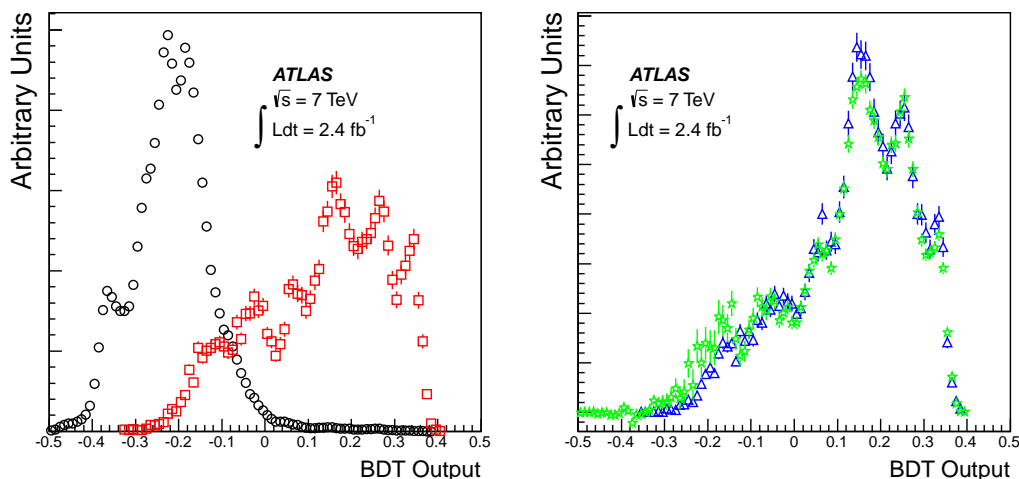


**Figure 1:** *Left:* BDT output for the background measured in  $B_s^0 \rightarrow \mu^+ \mu^-$  sideband data (circles) and the  $B_s^0 \rightarrow \mu^+ \mu^-$  signal MC (squares). *Right:* comparison of the BDT output between the  $B^\pm \rightarrow J/\psi K^\pm$  ( $J/\psi \rightarrow \mu^+ \mu^-$ ) signal MC (triangles) and the sideband-subtracted data (stars) samples, [6].

The agreement between the distributions of discriminating variables in data and MC has been verified on the  $B^\pm$  data (sideband-subtracted) and MC samples. The distributions of  $B$  meson kinematic variables  $p_1^B$  and  $\eta^B$  in MC were matched to the ones in data by applying a re-weighting technique. Additionally, due to the differences in  $b$  quark fragmentation processes between  $B_s^0$  and  $B^\pm$ , the distribution of the isolation variable was cross-checked on the  $B_s^0 \rightarrow J/\psi \phi \rightarrow \mu^+ \mu^- K^+ K^-$  data and MC samples. No significant disagreements have been found and the residual discrepancies between data and MC were taken into account as systematic uncertainties.

The implementation of Boosted Decision Trees (BDT) in the TMVA package [11] has been found to be the most powerful multi-variate analysis tool. The BDT output variable separates well the signal and the background, as seen in Figure 1 (*left*). A crosscheck on the  $B^\pm$  reference channel (by applying the same BDT weights) shows good agreement between the MC signal sample and the sideband-subtracted data (Figure 1, *right*). The BDT selection and the size of the mass search window  $\Delta m$  have been optimized in each mass resolution category by maximizing the estimator  $\mathcal{P} = \epsilon_{\text{sig}} / (1 + \sqrt{N_{\text{bkg}}})$  for 95% CL[12], where  $\epsilon_{\text{sig}}$  is the signal selection efficiency and  $N_{\text{bkg}}$  is the number of background events in the search region obtained by interpolation from the sidebands (using odd-numbered events only or 50% of the sample).

## 5. Results

The  $N_{J/\psi K^\pm}$  yield was computed by performing a binned maximum likelihood fit on the selected events. The systematic uncertainties on this yield were assessed by varying the bin size, the signal and background fit models, and by inclusion of the per-event mass resolution into the fit. The uncertainties on the yield are dominated by systematic uncertainties and equal to 2.9%, 7.4% and 14.1% for  $|\eta|_{\text{max}}$  intervals of 0-1, 1-1.5 and 1.5-2.5, respectively. The systematic (statistical) uncertainties on the  $\epsilon \times A$  ratio  $R_{\epsilon A}$  between the signal and the reference channels are 3.1 (3.1)%,

5.5 (4.8)% and 5.9 (5.3)%, correspondingly. The main source of the systematic uncertainty on the branching fraction, common to all resolution categories, is the ratio of  $b$ -quark fragmentation fractions  $f_u/f_s$  with 8% uncertainty [8]. Background scaling factors, defined as the ratio of continuous background events in the sidebands over those expected in the search region, have a common uncertainty of 4%. Other common sources of uncertainty are the absolute  $K^\pm$  reconstruction efficiency (5%), the difference of the vertex reconstruction efficiencies in data and MC (2%), and the asymmetry in the detector response to  $K^+/K^-$  (1%).

Table 1 summarizes all quantities required for the upper limit extraction: the SESs and their constituents, the background scaling factors, the number of events in the sidebands used for background interpolation, the estimated number of resonant background events and the number of observed events in the unblinded region for each resolution category. The unblinded di-muon invariant mass distributions are shown in Figure 2.

$ \eta _{\max}$ range	0–1.0	1.0–1.5	1.5–2.5
SES = $(\epsilon \epsilon_i)^{-1}$ [ $10^{-8}$ ]	0.71	1.6	1.4
$\epsilon = (f_s/f_u)/\mathfrak{B}(B^\pm \rightarrow J/\psi K^\pm \rightarrow \mu^+ \mu^- K^\pm)$ [ $10^3$ ]	$4.45 \pm 0.38$		
$\epsilon_i = N_{N_{J/\psi K^\pm}}^i / R_{\epsilon A}^i$ [ $10^4$ ]	$3.14 \pm 0.17$	$1.40 \pm 0.15$	$1.58 \pm 0.26$
bkg. scaling factor	1.29	1.14	0.88
observed in sideband regions $N_{\text{bkg}}^i$	5	0	2
expected resonant bkg. $N_{B \rightarrow hh}^i$	0.10	0.06	0.08
observed in search region $N_{\mu^+ \mu^-}^i$	2	1	0

**Table 1:** Single event sensitivities, background scaling factors and event counts in the three mass resolution categories. The SES constituents, expressed by a common to all resolution categories part  $\epsilon$  and a per-category part  $\epsilon_i$ , are also given together with their uncertainties. The quoted uncertainties combine in quadrature both statistical and systematic uncertainties. This table does not include the additional sources of common uncertainties described in the text. The  $N_{\text{bkg}}^i$  numbers are quoted for 50% of the sample (even numbered events only), [6].

The expected limit is calculated prior to unblinding by setting the number of events in the blinded region to the sum of the expected background events obtained by interpolation of the sidebands and the resonant background contribution. The expected limit is  $2.3_{-0.5}^{+1.0} \times 10^{-8}$  at 95% CL (in the given range 68% of the pseudo-experiments are found) and the observed limit is  $2.2 \times 10^{-8}$  at 95% CL [6].

## 6. Summary

An upper limit on the branching fraction  $\mathfrak{B}(B_s^0 \rightarrow \mu^+ \mu^-) < 2.2 (1.9) \times 10^{-8}$  at 95% (90%) CL has been set by the ATLAS detector using  $2.4 \text{ fb}^{-1}$  of data collected in 2011. The ATLAS result is used for calculation of the first LHC-wide combination result on the  $\mathfrak{B}(B_s^0 \rightarrow \mu^+ \mu^-)$  upper limit [13, 14].

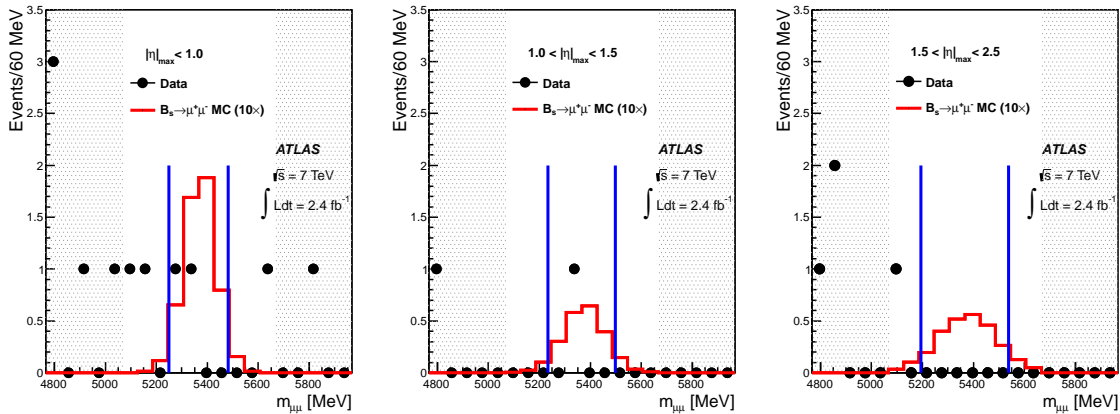


**Figure 2:** Number of candidates (dots) for each mass resolution category in the unblinded region (white areas) and in the sidebands (grey areas) in data as a function of di-muon invariant mass after applying all selection criteria. In each plot the vertical lines mark the optimized search window  $\Delta m$  and the continuous line - the MC prediction of the signal assuming  $\mathfrak{B}(B_s^0 \rightarrow \mu^+ \mu^-) = 3.5 \cdot 10^{-8}$ , [6].

## References

- [1] A. J. Buras *et al.*, *Higgs-mediated FCNCs: natural flavour conservation vs. minimal flavour violation*, JHEP **1010** (2010) 009.
- [2] D0 Collaboration, *Search for the rare decay  $B_s^0 \rightarrow \mu^+ \mu^-$* , Phys. Lett. B **693** (2010) 539-544.
- [3] CDF Collaboration, *Search for  $B_s^0 \rightarrow \mu^+ \mu^-$  and  $B^0 \rightarrow \mu^+ \mu^-$  Decays with CDF II*, Phys. Rev. Lett. **107** (2011) 191801.
- [4] CMS Collaboration, hep-ex/1203.3976, submitted to JHEP.
- [5] LHCb Collaboration, *Strong Constraints on the Rare Decays  $B_s^0 \rightarrow \mu^+ \mu^-$  and  $B^0 \rightarrow \mu^+ \mu^-$* , Phys. Rev. Lett. **108** (2012) 231801.
- [6] ATLAS Collaboration, *Search for the decay  $B_s^0 \rightarrow \mu^+ \mu^-$  with the ATLAS detector*, Phys. Lett. B **713** (2012) 387-407.
- [7] ATLAS Collaboration, *The ATLAS Experiment at the CERN Large Hadron Collider*, JINST **3** (2008) S08003.
- [8] LHCb Collaboration, *Measurement of  $b$  hadron production fractions in 7 TeV  $pp$  collisions*, Phys. Rev. D **85** (2012) 032008.
- [9] Heavy Flavor Averaging Group, *Averages of  $b$ -hadron,  $c$ -hadron, and tau-lepton properties*, arXiv:hep-ex/1010.1589v3.
- [10] A. Read, *Presentation of search results: The  $CL(s)$  technique*, J. Phys. G: Nucl. Part. Phys. **28** 2693, 2002.
- [11] *TMVA 4, Toolkit for Multivariate Data Analysis with ROOT, Users Guide*, tech. rep., CERN, arXiv:physics/0703039.
- [12] G. Punzi, *Sensitivity of searches for new signals and its optimization*, tech. rep., SLAC, Stanford, CA, 2003, arXiv:physics/0308063.

- [13] ATLAS, CMS and LHCb collaborations, *Search for the rare decays  $B_{(s)}^0 \rightarrow \mu^+ \mu^-$  at the LHC with the ATLAS, CMS and LHCb experiments*, ATLAS-CONF-2012-061 (<https://cdsweb.cern.ch/record/1456262>), CMS-PAS-BPH-12-009, LHCb-CONF-2012-017.
- [14] F. Archilli, these proceedings.